Annals of Nuclear Medicine Vol. 19, No. 3, 207–215, 2005

Three-dimensional registration of myocardial perfusion SPECT and CT coronary angiography

Hidenobu NAKAJO, Shin-ichiro KUMITA, Keiichi CHO and Tatsuo KUMAZAKI

Department of Radiology, Center for Advanced Medical Technology, Nippon Medical School

Objective: In this study, we describe a new technique for three-dimensional registration of CT coronary angiography (CTCA) and gated myocardial perfusion SPECT. ***Methods:*** Twelve patients with known or suspected CAD who underwent CTCA and gated SPECT were enrolled retrospectively. Coronary arteries and their branches were traced using CTCA data manually and reconstructed in three-dimensions. Gated SPECT data were registered and mapped to a left ventricle binary model extracted from CTCA data using manual, rigid and nonrigid registration methods. ***Results:*** Three-dimensional reconstruction and volume visualization of both modalities were successfully achieved for all patients. All 3 registration methods gave better quality based on visual inspection, and nonrigid registration gave significantly better results than the other registration methods ($p < 0.05$). The cost function for three-dimensional registration using nonrigid registration (235.3 ± 13.9) was significantly better than those of manual and rigid registration (218.5 ± 15.3 and 223.7 ± 17.0, respectively). Inter-observer reproducibility error was within acceptable limits for all methods, and there were no significant difference among the methods. ***Conclusion:*** This technique of image registration may assist the integration of information from gated SPECT and CTCA, and may have clinical application for the diagnosis of ischemic heart disease.

Key words: single photon emission computed tomography, three-dimensional registration, computed tomographic coronary angiography

INTRODUCTION

OBSERVATION AND UNDERSTANDING of pathophysiological conditions from various angles plays a very important role in diagnosis, clinical decision making, treatment, and determining disease prognosis. This is also true for patients with coronary artery disease (CAD). Recent advances in diagnostic procedures, imaging technology, and analysis capability has made it possible to use various techniques to observe pathophysiological conditions from many different angles. For the diagnosis of CAD, imaging modalities such as nuclear medicine imaging (SPECT and PET), ultrasonography and conventional X-ray coronary angiography (CAG) play a crucial role in the collection of a broad range of anatomical and physiological information for analysis. Additionally, recent reports have shown the usefulness of computed tomography (CT) and magnetic resonance imaging in the diagnosis and analysis of CAD.[1–5] Various kinds of information can be obtained from these imaging modalities, and there are various ways to display and interpret the information. Conventionally, cardiologists mentally integrated these various kinds of anatomical and physiological information into a three-dimensional or four-dimensional model. However, in order to perform a more objective analysis of data, the development of applications which can produce an integrated display of the results from the separate modalities is strongly desirable for diagnostic imaging. Studies using a technique which fuses images produced by nuclear medicine imaging with images produced by other modalities have been reported, but most of these reports deal with the central nervous system, and the technique has rarely been applied to cardiology.[6–9] For the diagnosis of CAD,

Received September 15, 2004, revision accepted January 11, 2005.

For reprint contact: Hidenobu Nakajo, M.D., Department of Radiology, Center for Advanced Medical Technology, Nippon Medical School, Sendagi 1–1–5, Bunkyo-ku, Tokyo 113–8603, JAPAN.

Table 1 Patient characteristics, cardiovascular risk factors and nuclear variables for 12 patients

	Value
Patient characteristics	
Age (yrs)	66 ± 9 (49–81)
Femal gender (*n*)	6 (50%)
History of AMI (*n*)	8 (67%)
History of PTCA (*n*)	7 (58%)
CAD risk factors	
Diabetes mellitus (*n*)	4 (33%)
Hyperlipidemia (*n*)	9 (75%)
Hypertension (*n*)	9 (75%)
SPECT MPI	
summed severity score	1.3 ± 2.4 (0–6)
extent score	0.7 ± 1.2 (0–3)
Interval between SPECT MPI and CTCA (days)	8 (2–14)

n = number of patients.
AMI; acute myocardial infarction, PTCA; percutaneous transluminal coronary angioplasty, CAD; coronary artery disease, SPECT MPI; single photon emission computed tomographic myocardial perfusion imaging, CTCA; computed tomographic coronary angiography

it is useful to fuse anatomical information (coronary tree) with physiological information (myocardial perfusion) because it is known that there are numerous variations in the anatomy of the coronary arteries. However, up until now, there have only been a small number of reports that describe the three-dimensional integration of coronary trees and myocardial perfusion information. Even in these reports, invasive CAG was used as a modality for determining the coronary arterial structure.[7,8] Recently, spiral scanning and multislice CT have been developed, and the usefulness of CT in cardiology, especially in visualizing the coronary arterial structure by CT coronary angiography (CTCA), has been investigated.[1,4,5] It is becoming possible to determine the coronary arterial structure without performing CAG. Based on this background, in the present study, we report the development of an application for the three-dimensional registration and fusion imaging of gated myocardial perfusion SPECT and CTCA.

MATERIALS AND METHODS

Study population

Between January 2003 and April 2004, we studied consecutive 12 patients (mean age of 66 ± 9 yo, six males, six females) with known or suspected CAD who underwent gated SPECT MPI and CTCA. Informed consent was obtained from all patients, who were examined using both gated SPECT MPI and CTCA within two weeks of each other. Between the procedures, there were no changes in clinical status, medical or surgical therapy, or any cardiac events or intervention. The patient characteristics are summarized in Table 1.

Gated SPECT data acquisition and analysis

Thirty to 40 minutes after an intravenous injection of 600 to 740 MBq of Tc-99m Sestamibi or Tc-99m tetrofosmin at rest, ECG-gated myocardial perfusion SPECT data acquisition was started with a 3-headed gamma camera (PRISM3000; Marconi Medical Systems, Inc., Ohio, USA) equipped with low-energy, general-purpose collimators. The gated SPECT data were acquired over 360 degrees in 20 (×3) steps, each of which consisted of 60 beats. Sixteen frames per R-R interval were acquired in a 64 × 64 matrix and a 15% window centered on the 140-keV photopeak of Tc-99m. The acceptance window was set at 20% during beat collection. All scanning was performed during quiet respiration without breath holding. Acquired SPECT data set was transferred to Odyssey FX workstation (Marconi Medical Systems, Inc., Ohio, USA). A Butterworth filter (order = 10, critical frequency = 0.2 cycles per pixel, slice thickness = 6.5 mm) was applied to the SPECT data and reconstruction was carried out using filtered back-projection with a ramp filter. Subsequently, reconstruction was reformatted into short-axis slices (matrix 64 × 64, slice thickness = 3.5 mm). Sequential four end-diastolic phase gated SPECT data set was summed and used for further analyses. In each patient, perfusion defect summed severity score and extent score were calculated using a method described in imaging guidelines for nuclear cardiology procedures.[10] The myocardial SPECT images of each patient were divided into 17 segments. This model uses three short-axis slices (apical, mid, and basal) to represent most of the ventricle and one vertical long-axis slice to better represent the left ventricular apex. The basal and mid short axis slices are divided into 6 segments and the apical short-axis slice is divided into 4 segments. A single apical segment is taken from the vertical long-axis slice. Two expert radiologists interpreted the SPECT images, and each segment was scored by consensus using a 5-point scoring system (0: normal perfusion, 1: mild reduction, 2: moderate reduction, 3: severe reduction, 4: absent uptake). The summed severity score is defined by the sum of the severity scores of all the segments. Defect extent score is expressed as the number of abnormal uptake segments.

CT coronary angiography data acquisition and reconstruction

CT examinations were performed by using a 16-detector row CT scanner (LightSpeed Ultra 16; General Electronic Medical Systems, WI, USA). For the contrast material-enhanced CT scanning, 80 mL of Iopamidol 370 mg I/mL was injected through a 20-gauge catheter into the right antecubital vein at 3 mL/sec followed by a 20-mL saline flush injection at the same rate of the contrast agent injection. An automated bolus-tracking technique (SmartPrep; General Electronic Medical Systems, WI, USA) was used for determining the contrast-enhanced scanning delay. This technique obtained real-time

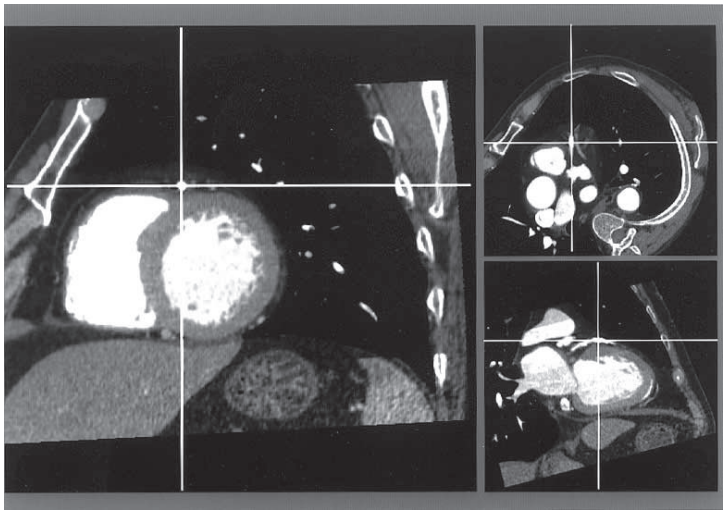

Fig. 1 Short-axis image (*left*) of CTCA is displayed to delineate each coronary artery. In addition to the short-axis images, corresponding horizontal long axis (*right top*) and vertical long axis (*right bottom*) images were displayed for reference.

Fig. 2 Extracted right and left coronary arteries overlaid on the CTCA images (*left column*: magenta points; operator-defined coronary artery, orange lines; spline interpolated coronary artery). Three-dimensional reconstruction coronary trees are displayed (*right column*: red curve, RCA; blue curve, LAD; white curve, LCx; yellow wired sphere, left ventricle).

Fig. 3 Three short axis slices of CTCA dataset (*top row*). Segmented epicardial and endocardial contours (*middle row*), and segmented LV binary model (*bottom row*).

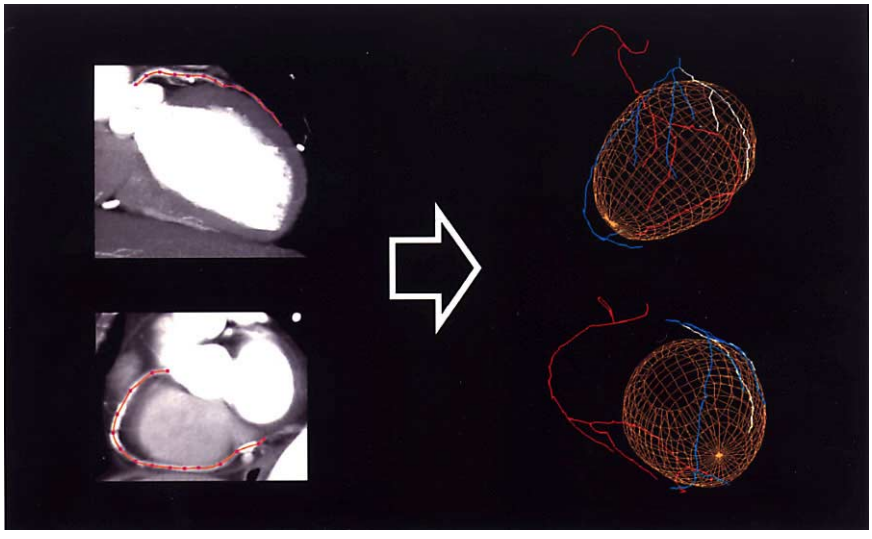

Fig. 2

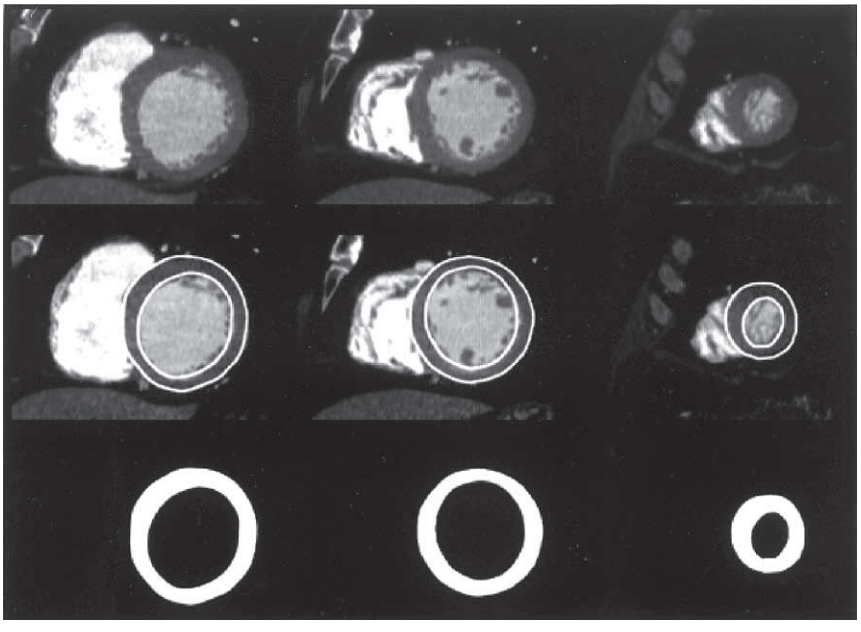

Fig. 3

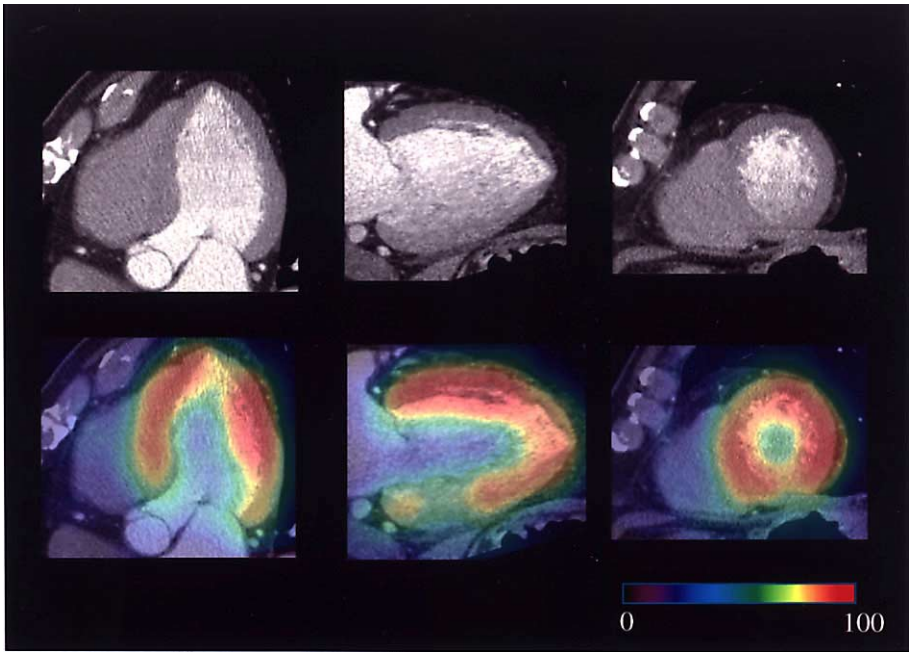

Fig. 4 Horizontal long, vertical long and short axis slices of CTCA images (*top row*). Registered SPECT images are overlaid on the CTCA images (*bottom row*).

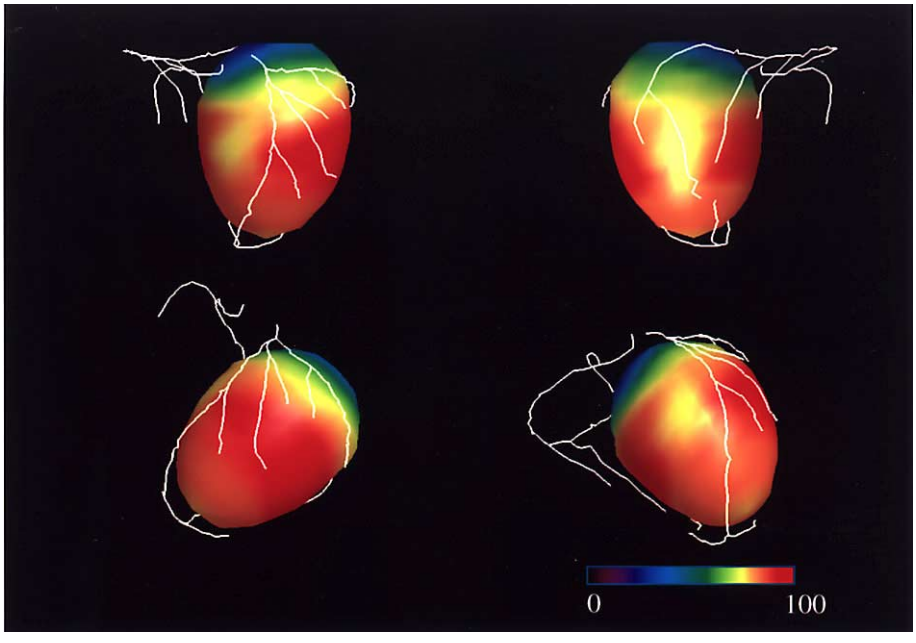

Fig. 5 An example of the final 3D registration and fusion images of SPECT and CTCA are displayed (*top left*; anterior view, *top right*; inferior view, *bottom left*; LAO view, *bottom right*; RAO view).

low-radiation-dose serial monitoring scans after the start of the injection of contrast material. The trigger threshold level was set at an increase of 100 Hounsfield Units above the baseline attenuation using a region of interest in the ascending aorta. After the trigger, CT scan was started. CT scans were obtained with a collimation of 16 × 0.625 mm, a pitch of 0.275 to 0.5 (automatically changeable with patient's heart rate), a rotation time of 500 msec, at 120 kV, and 350 mA while the ECG signal was recorded. Patients held their breath during the scan. Raw helical CT data were reconstructed to 0.625-mm thin section transverse CT images (matrix 512 × 512) in

the diastolic phase (70% of the R-R interval) with retrospective ECG gating.

Data analysis

Reconstructed images of both SPECT and CTCA data sets were transferred to a desktop computer-based workstation equipped with an Intel Pentium IV 2.8 GHz CPU and 1 GB RAM running Microsoft Windows platform for further analysis. The program code was written in IDL Version 6.0 (The Interactive Data Language from Research Systems, Inc., CO, USA) mainly. Some subroutines were coded in C and C++ languages. The software which we developed in the present study integrated three-dimensional images obtained from both modalities using the process described below.

Three-dimensional reconstruction of coronary tree using CTCA data

The transaxial CTCA images, which were transferred to the workstation, were reconstructed to short axis images of the left ventricle (LV), using an axis preset by an operator (Fig. 1). On the short axis CTCA images, an operator used a pointing device to define the center-points along its length for each coronary artery (Fig. 2). Additionally, for each arterial branch, the center-points in its course were defined. During this process, in addition to the short axis images, the vertical long axis and the horizontal long axis images were displayed for reference (Fig. 1). By using a spline function to connect these points along the length of each coronary artery, the 3D coronary tree was reconstructed (Fig. 2).

Segmentation of left ventricle using CTCA data

On the short axis CTCA images, the operator set the region of interest (ROI) to encompass the entire LV. The operator also defined the positions of the apex and the valve plane. When the set ROI is appropriate, its center is the LV cavity filled with contrast material. Therefore the LV cavity was segmented by expanding the center of the ROI (i.e., center of LV cavity) using the region growing method based on threshold range, followed by an ellipsoidal fitting. The surface of this ROI was defined as the endocardial surface. Then, this ROI was continuously and externally extended, and the epicardial surface was automatically extracted using the region growing method based on a multiplier of the standard deviation. These endocardial and epicardial surfaces, which had been defined by a computer with these processes, could be identified on the cross-sectional images. The operator may change the threshold and/or standard deviation multiplier value for the region growing method. As necessary, these surfaces were corrected manually by the operator. Using these processes, the LV wall data were extracted from the CTCA data, and were used as a LV binary model (Fig. 3).

Three-dimensional registration and display of LV binary model and SPECT

LV binary model and gated SPECT data were registered using manual, rigid and nonrigid registration methods. First, the voxel size of the SPECT data was adjusted to the voxel size of the CTCA data using a tri-linear interpolation. For manual registration, the CTCA was displayed on the screen and the SPECT data were superimposed on this mask (Fig. 4). The operator manually registered the SPECT data onto the CTCA using a pointing device. For rigid registration, 6 degrees of freedom (3 translations and 3 rotations) translation was used. Third order polynomial transformation following global affine transformation (12 degrees of freedom) was applied as a nonrigid registration[11] For automated rigid or nonrigid registration methods, SPECT data were registered onto an LV binary model instead of original CTCA images. The optimal transformation maximizes a cost function: $C(T) = 1/N \sum_{i=0 \text{ to } N-1} F(T \cdot r_i)$, where T is a geometrical transformation. $F(r)$ is the SPECT count value. A nonzero element of LV binary model is expressed as r_i, which contains N nonzero elements. Iterations are repeated until the cost function does not increase at a value less than the operator defined value.[12] After the three-dimensional registration of the SPECT data and the LV binary model (Fig. 4), we mapped the myocardial perfusion information onto the model of the left ventricular structure. First, the short axis images were prepared by dividing the LV binary model into 16 equal segments along the long axis from the apex to the base. Second, each short axis image was divided into 36 segments (10 degree angular increments from the center of the LV cavity). Therefore, the LV binary model was divided into 576 (16 × 36) polygonal surfaces. The information about myocardial perfusion in each polygonal surface was defined as the maximum count in the spatially registered SPECT images. Then, these polygonal surfaces were assembled to generate a three-dimensional left ventricular myocardial model which contained information about myocardial perfusion (Fig. 5).

Three-dimensional fusion display of coronary tree and myocardial perfusion

The three-dimensional coronary arterial structure and the three-dimensional left ventricular myocardial model, which were created using the above mentioned process, were displayed in three-dimensions. Since both were obtained from CTCA and had the same coordinates, further processing such as changing shapes and warping images was not performed.

Qualitative evaluation

Qualitative evaluations were performed by two experienced radiologists in consensus who had not been given any information about the patients.

Image quality of each coronary artery by CTCA was

evaluated visually by using a four-grade scoring system. Image quality was graded as follows: excellent quality, good quality (assessable for course and stenosis), fair quality (assessable for course, but nonassessable for stenosis) and poor quality (nonassessable for course or distribution). Segmentation quality of LV by CTCA was also evaluated visually using the four-grade scoring system: excellent quality. LV was successfully segmented without the need for parameter change; good quality, LV was segmented with interactive parameter change, fair quality; manual correction of LV boundary was needed, and poor quality; failure in LV segmentation.

For each registration method, the accuracy for the registration of the SPECT and the LV binary models were visually scored using the following four-grade scoring system (excellent quality, good quality, fair quality, and poor quality). This grading system was based on the following criteria (1: size, shape and position of the LV, 2: contour of LV wall, and 3: correspondence between SPECT count distribution and LV wall characteristics). Similar scoring was performed on the final 3D fused images of the SPECT MPI and the CT coronary tree.

Quantitative evaluation

We also compared the cost function for the registration of the LV binary model and the SPECT among the registration methods as a quantitative evaluation. The same radiologists independently performed 3D registration of the LV binary model and the SPECT MPI to evaluate inter-observer reproducibility error. SPECT data sets were sampled after registration to generate equally spaced intervals of 1000 points. These points were used to calculate the average distance between the two corresponding points in the two models.

Statistical analysis

All data were expressed as mean ± one standard deviation. To compare visual inspection with semiquantitative analysis for registration of the LV binary model and the SPECT MPI among the registration methods, a nonparametric analysis of variance was used. One-way repeated-measure analysis of variance was also used to compare the cost function for the registration. When statistical significance was noted, group comparisons were performed using Tukey's method. A p-value of less than 0.05 was considered significant.

RESULTS

All SPECT and CTCA data had adequate image quality for further analysis. Severity and extent score of the SPECT MPI were 1.3 ± 2.4 (range 0 to 6) and 0.7 ± 1.2 (range 0 to 3), respectively. That is to say that each patient had almost normal to mild hypoperfused myocardium, and no patient had severely and/or broadly hypoperfused myocardium. The segmentation of the LV and the coronary arteries was successfully performed for all patients. The time taken was approximately 30 ± 6 seconds (range 21 to 40) for extracting the LV binary model from CTCA data and 15–30 minutes for manual delineation of each coronary artery. The coronary tree and the extracted LV

Table 2 Image quality of each coronary artery by CT coronary angiography

Score	coronary arteries		
	RCA	LAD	LCx
Excellent	6	10	6
Good	4	2	5
Fair	2	0	1
Poor	0	0	0

RCA; right coronary artery, LAD; left anterior descending artery, LCx; left circumflex artery

Table 3 Comparisons of registration accuracy among the three registration methods

	Registration of SPECT onto LV			Final 3D fusion image		
	manual	rigid	nonrigid	manual	rigid	nonrigid
Score by qualitative evaluation*						
Excellent	5	5	10	4	4	9
Good	5	5	2	6	6	3
Fair	2	2	0	2	2	0
Poor	0	0	0	0	0	0
Cost function**	218.5 ± 15.3	223.7 ± 17.0	235.3 ± 13.9	–	–	–
Inter-observer reproducibility error (mm)†	2.1 ± 1.7	3.6 ± 2.5	2.2 ± 1.8	–	–	–

SPECT; single photon emission computed tomography, LV; left ventricle

* Significant differences observed for manual versus nonrigid registration ($p < 0.05$) and rigid versus nonrigid registration ($p < 0.05$). Comparisons performed by using a nonparametric analysis of variance.

** Significant differences observerd for manual versus rigid ($p = 0.005$), for manual and nonrigid ($p = 0.003$) and for rigid versus nonrigid registration ($p = 0.008$). Comparisons performed by using one-way repeated-measure analysis of variance.

† No significant differences among the registration methods.

binary model were of good quality in most patients (Table 2). The LV extraction score was excellent for 4 of 12 patients, good in 5, and fair in 3. No patient was graded with a poor segmentation. The observer needed to correct the LV edge manually in 3 patients. The errors observed in segmentation were attributed to the LV septal wall, hypertrophic papillary muscles, and thin portions of the myocardium such as infarcted area or apical regions.

The time needed for SPECT and LV binary model registration for manual, rigid and nonrigid registration were 68 ± 31 seconds (range 23 to 103), 8 ± 4 seconds (range 3 to 15) and 36 ± 11 seconds (range 20 to 52), respectively. For all three registration methods, the spatial registrations performed were generally good (Table 3).

Registration quality agreed in 6 of 12 patients between rigid and nonrigid registrations. Registration quality of nonrigid registration was superior to that of rigid registration in 6 patients, and in none of the cases was the quality of nonrigid registration inferior to that of rigid registration. Nonrigid registration was ranked significantly higher than the other two registration methods ($p < 0.05$). There was no significant difference between rigid and manual registration. Cost functions for manual, rigid and nonrigid registrations were 218.5 ± 15.3, 223.7 ± 17.0 and 235.3 ± 13.9, respectively. Cost function of nonrigid registration was significantly better than the other two registration methods ($p < 0.01$). Inter-observer reproducibility error for manual, rigid and nonrigid registrations were 2.1 ± 1.7 mm, 3.6 ± 2.5 mm, and 2.2 ± 1.8 mm, respectively. There was no significant difference among the 3 registration methods. The time taken for the three-dimensional display of the coronary trees and myocardial perfusion was one second or less. The results of the visual interpretation on the final fused images of SPECT and the coronary arterial structure are shown in Table 3. In the 12 patients who were assessed, these results were generally good, and three-dimensional fusion of the myocardial perfusion SPECT and CTCA images could be performed (Fig. 5).

DISCUSSION

In the present study, we have developed a technique for the semi-automatic three-dimensional fusion of anatomical information (coronary tree obtained from CTCA) and physiological information (myocardial perfusion SPECT). We applied this technique to patients with coronary artery disease and were able to create satisfactory fused images in all patients. Thus far, a number of reports in which three-dimensional display and fusion of images have been attempted have dealt mainly with the central nervous system, but there have been few reports of its use in cardiology. There are several reasons for this. First of all, the brain is stable in the skull and does not move during examination. In contrast, during respiration the heart moves by the motion of the diaphragm and the thoracic cage, and itself beats. Moreover, the organs in the thoracic cage change shape according to body position and the shape of the examination table on which a patient is lying. Second, compared to the brain, the heart does not have many anatomical landmarks. For the central nervous system, attempts have been made to use external fiducial markers to perform positioning.[13] However, this is not efficient in cardiology, since respiratory motion causes the movement of external fiducial markers adjusted to the thoracic cage. Consequently, in cardiology, three-dimensional image fusion is technically difficult, but is still required. In this study, we employed nonrigid transformation for the three-dimensional registration to resolve these problems. Our results suggested that manual, rigid and nonrigid registration methods gave generally good registration quality. However, nonrigid registration gave more reliable results.

Many studies have been conducted regarding the detection of CAD with SPECT MPI using a model with assumed coronary artery distribution.[14,15] Such studies validated a 17-segment polar map by comparing the predefined coronary territory assignment with the actual angiographically derived coronary distribution.[16] They concluded that, for major epicardial coronary arteries, both the sensitivity and specificity of SPECT MPI for the detection of CAD are better when using anatomical matching rather than the model-based approach. Consequently, combining image information for each individual improves diagnostic accuracy in clinical practice. In the present study, we did not plot the fused data onto the two-dimensional polar coordinates shown above, but we produced a three-dimensional integrated display of the data. Therefore, it may be possible to attain undistorted fusion that can be intuitively understood.[17–19]

There are a small number of reports in which the three-dimensional fusion of the coronary arterial structure and myocardial perfusion has been attempted.[7,8] However, in these reports, CAG was used for obtaining the coronary arterial structure. Therefore, this is the first report describing the fusion of CTCA and SPECT. Although CAG is still the gold standard for the detection and quantification of CAD, it is an expensive and invasive procedure. In contrast, CTCA is considerably less invasive and less expensive. Additionally, spatial distortion occurs with CAG, since data from biplane projections are used for the three-dimensional reconstruction of the coronary arterial structure. Moreover, coronary angiographic data do not contain spatial information about left ventricular structure, so when coronary trees reconstructed from CAG are registered onto SPECT MPI, the operator needs to carry out manual positioning based on anatomical landmarks such as the atrioventricular groove. On the other hand, data containing undistorted three-dimensional information can be obtained from CTCA. Since data from CTCA are used for creating a model of the myocardial structure of the LV, processes such as moving images and changing shapes are not necessary. Therefore, the fusion of CTCA

and SPECT is considered to be an excellent method in terms of reduced spatial distortion and reproducibility. However, regarding spatial and temporal resolution, CTCA is inferior to CAG, so is not by itself sufficient for detecting coronary artery stenoses, and cannot be a substitute for CAG.[20] Therefore, in the present study, we decided to use CTCA to determine the paths of the coronary arteries, and the principle purpose was to obtain a three-dimensional relationship between the distribution of myocardial perfusion and the area covered by the coronary arteries.

Recently, vulnerable or unstable plaques have been attracting attention as a cause of acute coronary syndrome. Acute coronary syndrome often results from rupture of a modestly stenotic vulnerable plaque, not visible by conventional CAG.[21] Consequently, for diagnosis and analysis of CAD, it is necessary to detect not only the significant stenosis, but also the characteristics of the nonstenosed vessels and the vascular lumen. Schroeder et al.[22] reported that less invasive CTCA showed good diagnostic accuracy with regard to lesion detection and quantification compared to intracoronary ultrasound as a gold standard for *in vivo* plaque detection. We did not examine coronary lesions, such as plaques, in the present study. However, it is expected that by developing the detection and display of coronary lesions, in addition to assessment of the anatomical path of the coronary arteries and the diameters of vessels, it will become possible to perform a more physiological assessment of the myocardium, which could not be obtained from CAG alone.

The present study had several limitations. First, the number of subjects studied was small (12 patients). Satisfactory results were obtained in all patients in whom three-dimensional fusion was performed. However, we did not examine patients with a broad perfusion defect or patients with multivessel disease. For such cases, we should validate registration accuracy using non-gated SPECT instead of gated SPECT. It is important to validate the clinical diagnostic efficiency of this technique in a larger cohort of patients. We also should apply this technique not to rest SPECT but stress SPECT MPI. Second, in this study the coronary arterial structure was manually extracted by an operator from the CTCA, which was time consuming. Volume and surface rendering techniques are conventionally used for three-dimensional reconstruction, and their reproducibility and processing speed are high. However, the diameters of the coronary arteries are very small, and they are tortuous. Moreover, the LV cavity and the coronary sinus, which are strongly enhanced, are adjacent to the coronary arteries. Therefore, with these techniques, which use CT values, it is difficult to project images of the coronary arteries with sufficient length and to obtain images of fine branches. In the near future, the development of new automatic reconstruction methods, which utilize artificial intelligence or a priori knowledge database, will make it possible to perform a more objective and reproducible assessment. However, at present, we considered that the best technique was to have an operator manually define the coronary arteries, even though it was time consuming.

Recently, assessments of the LV regional wall motion and wall contractility are commonly performed using gated SPECT. Many papers have reported that ECG-gating may improve the accuracy of diagnosis of CAD.[14,23–25] In the future, we plan to develop an integrated approach that includes functional imaging such as analysis of LV regional wall motion.

In conclusion, we have developed a new application for three-dimensional registration of myocardial SPECT and CTCA data. This approach enables us to perform three-dimensional fusion of data from different sources and thus facilities observation of integrated physiological information (myocardial perfusion) and anatomical information of the coronary arteries. This fusion technique was less distorted than conventionally reported techniques. We propose to use this procedure with a larger number of patients in order to evaluate its diagnostic efficiency.

ACKNOWLEDGMENTS

The authors would like to thank Dr. Hiromitsu Hayashi for his support in providing the CTCA data used in this study, and Dr. Susumu Okada for his help in preparing this manuscript.

REFERENCES

1. Schroeder S, Kopp AF, Baumbach A, Kuettner A, Herdeg C, Rosenberger A, et al. Noninvasive detection of coronary lesions by multislice computed tomography: results of the new age pilot trial. *Cathet Cardiovasc Intervent* 2001; 53: 352–358.
2. Gerber TC, Kuzo RS, Lane GE, O'Brien PC, Karstaedt N, Morin RL, et al. Image quality in a standardized algorithm for minimally invasive coronary angiography with multislice spiral computed tomography. *J Comput Assist Tomogr* 2003; 27: 62–69.
3. Choudhury RP, Fuster V, Badimon JJ, Fisher EA, Fayad ZA. MRI and characterization of atherosclerotic plaque: emerging applications and molecular imaging. *Arterioscler Thromb Vasc Biol* 2002; 22: 1065–1074.
4. Kopp AF, Schroeder S, Baumbach A, Kuettner A, Georg C, Ohnesorge B, et al. Non-invasive characterisation of coronary lesion morphology and composition by multislice CT: first results in comparison with intracoronary ultrasound. *Eur Radiol* 2001; 11: 1607–1611.
5. Mahnken AH, Wildberger JE, Sinha AM, Dedden K, Stanzel S, Hoffmann R, et al. Value of 3D-volume rendering in the assessment of coronary arteries with retrospectively ECG-gated multislice spiral CT. *Acta Radiol* 2003; 44: 302–309.
6. Faber T, McColl R, Opperman R, Corbett J, Peshock R. Spatial and temporal registration of cardiac SPECT and MR images: methods and evaluation. *Radiology* 1991; 179: 857–861.
7. Peifer JW, Ezquerra NF, Cooke CD, Mullick R, Klein L, Hyche ME, et al. Visualization of multimodality cardiac

imagery. *IEEE Trans Biomed Eng* 1990; 37: 744–756.
8. Schindler TH, Magosaki N, Jeserich M, Oser U, Krause T, Fischer R, et al. Fusion imaging: combined visualization of 3D reconstructed coronary artery tree and 3D myocardial scintigraphic image in coronary artery disease. *Int J Card Imaging* 1999; 15: 357–368.
9. Sturm B, Kimerly A, Powell, Arthur ES, Richard DW. Registration of 3D CT angiography and cardiac MR images in coronary artery disease patients. *Int J Card Imaging* 2003; 19: 281–293.
10. Cerqueira MD, Weissman NJ, Dilsizian V, Jacobs AK, Kaul S, Laskey WK, et al. Standardized myocardial segmentation and nomenclature for tomographic imaging of the heart: a statement for healthcare professionals from the cardiac imaging committee of the council on clinical cardiology of the American heart association. *Circulation* 2002; 105: 539–542.
11. Woods RP. Spatial transformation models. In: *Handbook of medical imaging processing and analysis*, Bankman IN (ed), San Diego; Academic Press, 2000: 465–497.
12. Herk MV. Image registration using chamfer matching. In: *Handbook of medical imaging processing and analysis*, Bankman IN (ed), San Diego; Academic Press, 2000: 515–527.
13. Barnden L, Kwiatek R, Lau Y, Hutton B, Thurfjell L, Pile K, et al. Validation of fully automatic brain SPET to MR co-registration. *Eur J Nucl Med* 2000; 27: 147–154.
14. Nakajo H, Kumita S, Mizumura S, Cho K, Kijima T, Kumazaki T, et al. Assessment of left ventricular contraction abnormalities with myocardial infarction using gated technetium-99m sestamibi SPECT: comparison of wall thickening and regional ejection fraction analysis for the detection of coronary artery stenosis. *KAKU IGAKU (Jpn J Nucl Med)* 1999; 36: 435–443.
15. Sharir T, Berman DS, Waechter PB, Areeda J, Kavanagh PB, Gerlach J, et al. Quantitative analysis of regional motion and thickening by gated myocardial perfusion SPECT: normal heterogeneity and criteria for abnormality. *J Nucl Med* 2001; 42: 1630–1638.
16. Schwartz JG, Johnson RB, Aepfelbacher FC, Paeker JA, Chen L, Azar RR, et al. Sensitivity, specificity and accuracy of stress SPECT myocardial perfusion imaging for detection of coronary artery disease in the distribution of first-order branch vessels, using an anatomical matching of angiographic and perfusion data. *Nucl Med Commun* 2003; 24: 543–549.
17. Biedenstein S, Schafers M, Stegger L, Kuwert T, Schober O. Three-dimensional contour detection of left ventricular myocardium using elastic surfaces. *Eur J Nucl Med* 1999; 26: 201–207.
18. Faber TL, Cooke CD, Peifer JW, Pettigrew RI, Vansant JP, Leyendecker JR, et al. Three-dimensional displays of left ventricular epicardial surface from standard cardiac SPECT perfusion quantification techniques. *J Nucl Med* 1995; 36: 697–703.
19. Henri CJ, Peters TM. Three-dimensional reconstruction of vascular trees. Theory and methodology. *Med Phys* 1996; 23: 197–204.
20. Achenbach S, Daniel WG. Noninvasive coronary angiography—An acceptable alternative? *N Eng J Med* 2001; 345: 1909–1910.
21. Falk E, Shah PK, Fuster V. Coronary Plaque Disruption. *Circulation* 1995; 92: 657–671.
22. Schroeder S, Kopp AF, Baumbach A, Meisner C, Kuettner A, Georg C, et al. Noninvasive detection and evaluation of atherosclerotic coronary plaques with multislice computed tomography. *J Am Coll Cardiol* 2001; 37: 1430–1435.
23. Germano G, Erel J, Lewin H, Kavanagh PB, Berman DS. Automatic quantitation of regional myocardial wall motion and thickening from gated technetium-99m sestamibi myocardial perfusion single-photon emission computed tomography. *J Am Coll Cardiol* 1997; 30: 1360–1367.
24. Kumita S, Cho K, Nakajo H, Toba M, Kijima T, Mizumura S, et al. Serial assessment of left ventricular function during dobutamine stress by means of electrocardiography-gated myocardial SPECT: combination with dual-isotope myocardial perfusion SPECT for detection of ischemic heart disease. *J Nucl Cardiol* 2001; 8: 152–157.
25. Choi J, Lee K, Kim S, Kim S, Kim B, Lee S, et al. Gating provides improved accuracy for differentiating artifacts from true lesions in equivocal fixed defects on technetium 99m tetrofosmin perfusion SPECT. *J Nucl Cardiol* 1998; 5: 395–401.